Wojciech TARNAWSKI[*], Marek KURZYŃSKI[*]

AN IMPROVED DIFFUSION DRIVEN WATERSHED ALGORITHM FOR IMAGE SEGMENTATION OF CELLS

The image segmentation is one of the most crucial steps in automated analysis of medical and biological images. The segmentation process allows for a detection of object contours. Due to specificity of imaging technique, a correct detection of cell contours is problematic because of the fuzzy and broken edges. Moreover, the cells are very often connected. The modified watershed algorithm based on the diffusion model presented in this paper has been successfully applied to segmentation of cells where the mentioned difficulties appear. The method was tested in contact endoscopy, a novel technique in the diagnosis of the larynx.

1. INTRODUCTION

Image segmentation of cells is a process of grouping an image pixels into significant regions denoting the cells. It is known as one of the basic, but very "cell-dependent" procedure because of the noise, and specific, ambiguous cell appearance in the raw images.

The segmentation method presented in this paper consists of two main steps: an image enhancement step, based on a nonlinear diffusion process generating an *activity image*, and followed by a modified watershed segmentation step. In the contrary to [9], we propose a novel definition of the activity image. Instead of considering an activity image as a three-dimensional surface, we propose a novel approach where the activity image reflects the *degree of diffusion*. It assumes *high values* in the vicinity of blurred edge pixels with low gradient, and *the low values* where the diffusion process does not introduce great changes in pixel values i.e. for interior pixels. In the case of strong edges with high gradient values (for example: between nuclei and cytoplasm) the diffusion process is inhibited and the degree of diffusion tends to zero. In the watershed segmentation step the activity image is fed through a modified watershed algorithm. In our case the activity image is considered as a topographic surface where the lines corresponding to the "mountains" (reflecting to fuzzy edges of cells) on the surface delineate the segments (cells) in the segmented image. The modified watershed algorithm takes advantage of the activity image and conceptually is derived from the geodesic reconstruction originally developed by Beucher [2] and later modified by Najman et al. [8]. The basic idea presented in these papers is to use the flooding principle developed by Vincent [11]. The new approach presented in this paper

[*] Chair of Systems and Computer Networks, Technical University of Wroclaw, Wyb. Wyspianskiego 27, 50-370 Wroclaw, Poland, e-mail:wojciech.tarnawski@pwr.wroc.pl

assumes that the activity image is an input image *f* which is "reconstructed" by flooding the catchment basins of *f* until they overflow, or until $\bar{f}$ (negative of image *f*) is achieved, which is also simultaneously flooded by the Vincent's watershed algorithm.

The method was tested on images from contact endoscopy that visualizes cells of the larynx. Similarly to other imaging techniques, such as phase contrast microscopy or bright field microscopy, the main challenge lies in a proper segmentation of cells and nuclei despite of their ambiguous appearance that results in *fuzzy and broken* cell membranes and nuclei envelopes (see Fig. 2).

The following structure of this paper is organized as follows. In the next section the concept of non-linear diffusion is presented. The following section consists of two subsections. The first presents the "cell model" and discusses the construction of the activity image. The second one describes a modified watershed algorithm used for cell detection. In the last section the experimental results and few conclusions are drawn.

2. DIFFUSION MODEL

In physics, diffusion processes govern the transport of heat, matter, and momentum leading to an increasing equalization of spatial concentration differences. In image processing the diffusion model can be adopted by treating the changes of grey or colour values of the pixel located at spatial coordinates (x, y) as local concentrations or, more precisely, as the feature vector $\vec{c}$ of a pixel value. Each component of the feature vector corresponds to the "concentration of diffusing pixels". In every time step some fraction of grey or colour value is exchanged with the neighbouring pixels according to formula [7]:

$$\frac{\partial \vec{c}(x, y)}{\partial t} = D(x, y)\Delta \vec{c}(x, y) + (c_0 - c) \cdot \eta(x, y) \tag{1}$$

where $D(x, y, t)$ denotes the inhomogenous diffusion coefficient:

$$D(x, y) = 1 - \exp\left(-\frac{\partial_m}{\left[\Psi_{M, s, d}\left(\|\nabla(B \otimes I(x, y)\| / \lambda\right)\right]^m}\right) \tag{2}$$

$\eta(x, y)$ stands for the exchange rate with reference concentration c_0. λ is an adjustable parameter. For low gradients $\|\nabla I(x, y, t)\| << \lambda$, D approaches *1*; for high gradients $\|\nabla I(x, y, t)\| >> \lambda$, D tends to zero. The δ_m parameter and exponent *m* control steepness of the exponential (soft) threshold. The linear operator *B* denotes smoothing filter convolved with image $I(x, y)$ at scale *t*. In our approach a standard diffusion model ($\eta = 0$) is assumed resulting in:

$$\frac{\partial \vec{c}(x, y, t)}{\partial t} = D(x, y)\Delta \vec{c}(x, y, t) \tag{3}$$

δ_m and m values were set similarly to Weickert [13] to $m = 4$ and $\delta_m = 3.31488$, respectively. The $\Psi_{M,s,d}$ function denotes a sigmoidal quasi-thresholding filter of a form:

$$\Psi_{M,s,d}(\alpha) = sY_{M,s,d} \cdot \left(\tan^{-1}\left(\frac{\alpha - d}{s} \right) + dY_{s,f} \right),$$

$$dY_{s,d} = \tan^{-1}\left(\frac{d}{s} \right), \qquad sY_{M,s,d} = \frac{M}{\frac{\pi}{2} + dY_{s,d}} \tag{4}$$

The parameter M denotes maximum value that can be obtained after applying a filter, s controls steepness of a sigmoidal "step" and d governs the shift. These three parameters decrease small values ($d > 0$) while taking greater values nonlinearly normalized up to a given value M.

The spatio-temporal discretisation of the model can be done with the use of simple explicit 1st order scheme which describes the concentration change at the pixel located in a position *(m,n)* at time *k+1* :

$$c_{n,m}^{k+1} = c_{n,m}^{k} + (c_{n+1,m}^{k} - 2c_{n,m}^{k} + c_{n-1,m}^{k})\varepsilon_{n,m}^{x} + (c_{n,m+1}^{k} - 2c_{n,m}^{k} + c_{n,m-1}^{k})\varepsilon_{n,m}^{y} \tag{5}$$

where $\varepsilon_{n,m}^{x}$ and $\varepsilon_{n,m}^{y}$ are discrete coefficient described as: $\varepsilon_{n,m}^{x} = \frac{D_{n,m}\Delta t}{\Delta x^2}$, $\varepsilon_{n,m}^{y} = \frac{D_{n,m}\Delta t}{\Delta y^2}$.

Linear smoothing filter B and the non-linear "flattening" function $\Psi_{M,s,d}$ are dedicated to improve the stability of the simple explicit scheme which is sensible to local discontinuities and sharp edges. The $\Psi_{M,s,d}$ filter can "select" only those edges which are sufficiently important. For computing the gradient map described in Eq. 2 by the $\|\nabla(B \otimes I(x,y,t)\|$ module the Canny edge detector [4] was used. In practice, modification of pixel values, expressed by Eq. 5, is repeated $q = 30$ times.

3. SEGMENTATION ALGORITHM

3.1. DEFINITION OF THE ACTIVITY IMAGE

The blurred and broken edges of cells make it impossible to precisely detect the cell contours with a classical watershed approach. For better visualization and later considerations let us create the "cell model" with centrally located nucleus, by suitably "modulated" inverse 2D Gaussian kernel whose values are presented as the grey values in Fig. 1.

The approach proposed in this paper assumes that the activity image "reflects" the *degree of diffusion*, or more precisely - the degree of local concentration changes described as the feature vector $\vec{c}$ for every point (pixel) of the analysed image. Hence, the *high values* reflect the neighbourhood of fuzzy edge pixels with low gradient, and the *low values* reflect image points where the diffusion process is slower or inhibited. The amount of diffusion

$\Delta S(x, y, t)$ for one image point located at spatial coordinates (x, y) up to scale t is expressed by the formula:

$$\Delta S(x, y, t) = \int_t \left[I(x, y, t) - I(x, y, t - \Delta t) \right] dt \qquad (6)$$

where $I(x, y, t)$ denotes pixel value after the diffusion-based filtering at scale t and $I(x, y, t - \Delta t)$ denotes pixel value at the previous scale value equal to ($t - \Delta t$). At scale $t = 0$ $I(x, y, t = 0)$ denotes pixel values being either negative or original, in the case of the bright cells on the dark background. In practice, differences between pixel values for increasing scales t are normalized according to the formula:

$$\Delta S(x, y, t) = \int_t \left[\frac{\left((I(x, y, t) - I(x, y, t - \Delta t)) + |\min(\Delta S_t)| \right)}{\max(\Delta S_t) - \min(\Delta S_t)} \right] dt \qquad (7)$$

Where $\max(\Delta S_t), \min(\Delta S_t)$ denote maximal and minimal difference $I(x, y, t) - I(x, y, t - \Delta t)$ at scale t. The diffusion process is stopped when $\max(\Delta S_t) - \min(\Delta S_t) \le \gamma$ where γ is user-defined value(for real images γ was set to 2).

The resulting activity images of the cell model are presented in Fig. 1. The value of q, that denotes the number of iterations for process described by Eq. 5 depends on the "fuzziness" of a cell membrane i.e. the fuzzier border edge the higher values of q.

As it is illustrated in Fig. 1, high values reflect the neighbourhood of fuzzy edge pixels presented at the border of the cell model while low nuclei values indicated where the changes corresponding to degree of diffusion are minimal. In the case of stronger edges (i.e. between dark an bright regions) it is interesting that pixels in the activity image are "attracted" to real image regions yielding sharper image edges, which later implies a better segmentation of nuclei for the watershed algorithm.

3.2. THE MODIFIED WATERSHED ALGORITHM

To obtain the actual segmentation of cells, the new approach for the watershed algorithm is presented. It is applied to the activity image that is obtained when the non-linear diffusion process is stopped. In our case, the activity image is considered as a topographic surface where the lines corresponding to the "mountains" on the surface delineate the segments (cells) in the segmented image. The modified watershed algorithm presented in this paper takes advantages of the activity image. Conceptually it is derived from Beucher-Meyer principle [2,3] called the waterfall algorithm which relies on the geodesic reconstruction by erosion. It is needed to stress that the proposed solution should not be considered "the modified geodesic reconstruction algorithm" as it uses the concept of flooding under some constraints presented in the [2,8].

The basic idea is to use the flooding principle developed by Vincent [11]. This principle is adapted to the geodesic reconstruction of activity image f under $\bar{f}$, where $\bar{f}$ denotes complement (negative) of f. f and $\bar{f}$ are flooded simultaneously and in the morphological terminology we would say that the activity image f is "eroded" under the

"dilated" f . It means that the watersheds produced on the image $\bar{f}$ become "important" only when they meet watersheds from f . This way we can reconstruct f by flooding the catchment basins of f until they overflow, or until the watersheds of $\bar{f}$ are met. When we flood the catchment basins of f flooding is stopped until one of their saddle points (contact point between two basins) are reached. In this case two cases of watersheds are possible:

- the height of flooding on f reaches the height of flooding on $\bar{f}$; this saddle is the contact point (watershed point) between basin on f and basin on $\bar{f}$,
- the saddle point between two basins of f is reached,

The segmentation algorithm presented in this paper based on the activity image consists of two steps. First, the activity image is rescaled linearly to the full range of grey values. This will form a number of "lakes" on the topographic landscape which reflect the whole cells. In the case of the cell segmentation it "improves" topographic landscape for the proposed watershed algorithm. This can be explained by the fact that maximal values in the activity image are present in the neighbourhood of blurred edge pixels with low gradient (cell borders), and the lowest values where the diffusion process is inhibited i.e. for cells interior pixels. More importantly, the watershed algorithm does not need the regional minima (or markers) as an input. The watershed algorithm starts flooding from the minima that correspond to cells on the image. By flattening the cell interior this step make nuclei disappear. Therefore, for the nuclei detection procedure this step is omitted.

In the second step, the rescaled activity image undergoes the presented, modified watershed algorithm.

The results of the cell and nuclei segmentation for the two artificial models with one (lower row) and two (upper row) cells are presented in the last column in Fig. 4. The second column includes the images presenting the degree of diffusion for input images, the third one column depicts the activity images after linear scaling. The parameter values for the images presented in Fig. 4 are the following: $q = 10$, $\Delta t = 0.08$ for the cell segmentation and $\Delta t = 0.03$ for the nuclei segmentation.
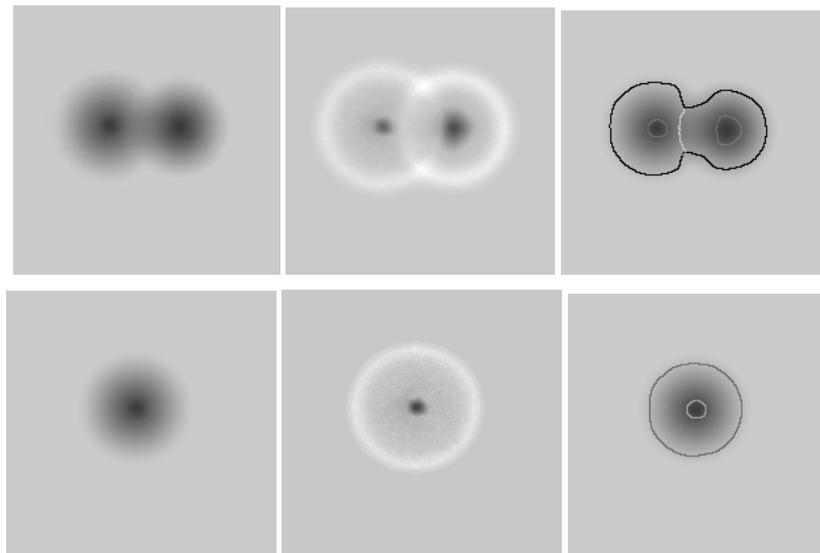
Fig.1. The results of cell and nuclei segmentation for artificial images with one cell (upper row) and two cells (lower row). Left column represents cell model (2D Gaussian kernel), middle – the activity image, and right – results of the segmentation.

3.3. CELL AND NUCLEI SEGMENTATION IN CONTACT ENDOSCOPY

The contact endoscopy has been extensively used in gynaecological, and more recently to visualize laryngeal and nasal tissues [1,12]. Preliminary experiences with contact endoscopy were realized in co-operation with the Department of Otolaryngology of the Wroclaw Medical University in Poland. They used Karl Storz 8715 BA contact endoscope guided down by the Kleinsasser laryngoscope towards the larynx until the exact area of interest was contacted. The main difficulties of contact endoscopy are related to diagnostic interpretation of the standard PAL-video signal. Therefore, for better interpretation and evaluation high-resolution images were captured and analysed with image processing and analysis methods. The prototype imaging system was constructed from 7 MPixels C-7070 Wide Zoom Olympus camera equipped with a specially constructed converter connected with a Karl Storz 8715 BA contact endoscope and Storz Xenon 300 lamp. As the whole system should be used during a surgery investigation, it was fully automated. Preliminary experiences indicated that the main problem was an objective diagnostic interpretation of resulting images (c.f. Fig. 2). Also, not enough medical experiments were performed, to draw statistically valuable results of the segmentation method.
Fig. 2 shows an example of images clipped from the original one as well as the segmentation results. The image analysis algorithm should also provide information required to evaluate detected cell structures: i.e. the presence of nuclei, their size, colour or intensity, the nucleus/cytoplasm ratio, shape properties of nuclei and cytoplasmic contours.

Initial experiments indicated that both the cells and the nuclei were successfully segmented by the proposed algorithm. The cell segmentation results were positively verified by the pathologist. The nuclei segmentation failed in some cases has failed, probably due to high cell degradation because the pathological nuclei are bigger and occupy almost the whole cell. In the future work, we would like to limit this defect. by running the proposed algorithm locally, i.e. independently for every previously detected cell.

4. CONCLUSIONS

In this paper the novel technique for segmentation of cells and nuclei based on the diffusion driven watershed algorithm is presented. To handle the problems with blurred and broken cell membranes and nuclei envelopes, the new concept of the activity image based on diffusion model was presented. In watershed segmentation step the activity image undergoes a modified watershed algorithm which takes into account the specificity of the rescaled activity images. These features were used for proper segmentation of cells and nuclei on images from contact endoscopy.
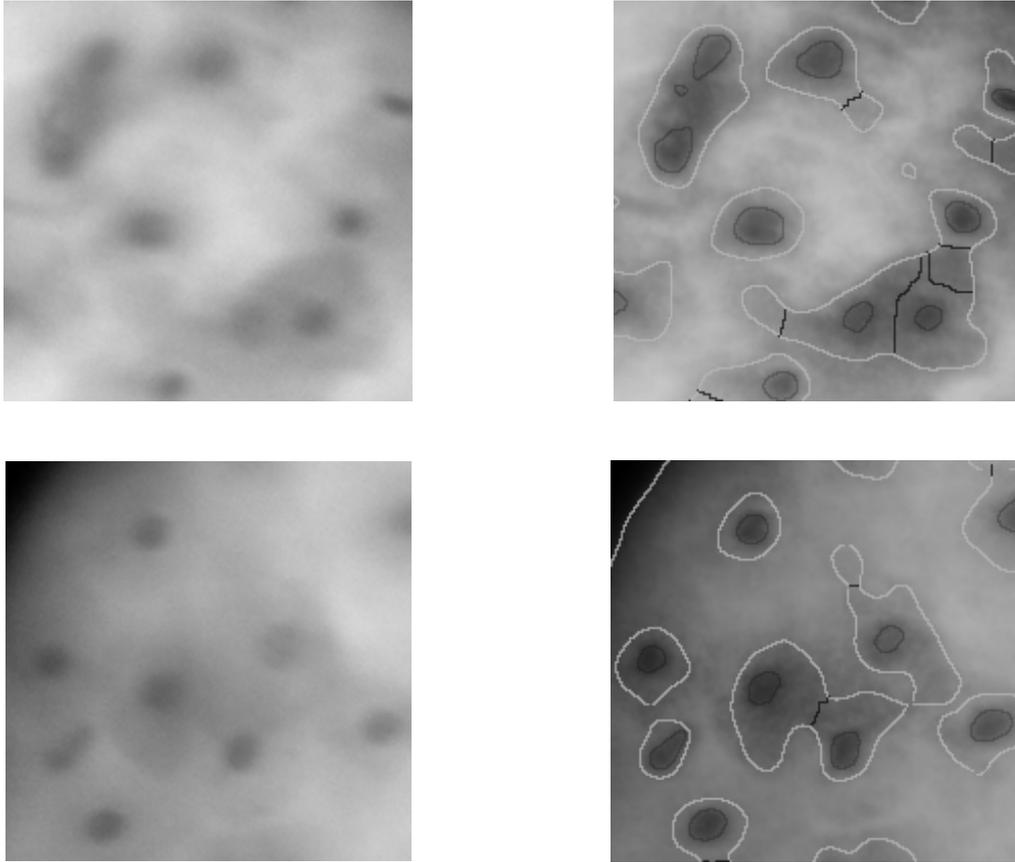
Fig.2. The results of cell segmentation (right) of the input images (left).

ACKNOWLEDGMENTS

BIBLIOGRAPHY

[1] ANDREA M, DIAS O, SANTOS A. Contact endoscopy during microlaryngeal surgery: a new technique for endoscopic examination of the larynx. Ann Otol Rhinol Laryngol,May; 104(5), pp. 333-339, 1995.

[2] BEUCHER S. AND F. MEYER, The Morphological Approach to Segmentation: The Watershed Transformation, Mathematical Morphology in Image Processing, E.R. Dougherty, ed., Optical Engineering, pp. 433-482, 1993.

[3] BEUCHER S. Watershed, hierarchical segmentation and waterfall algorithm, In: Math. Morphology and Its Appl. to ImageProcessing), pp. 69–76, 1994.

[4] CANNY J.F., A Computational Approach to Edge Detection, Readings in Computer Vision: Issues, Problems, Principles and Paradigms, MA. Fischler and 0. Firschein, eds., pp. 184-203, 1986.

[5] HIEU T. NGUYEN , QIANG JI, Improved watershed segmentation using water diffusion and local shape priors, Proceedings of the 2006 IEEE Computer Society Conference on Computer Vision and Pattern Recognition (CVPR'06)

[6] JAIN A. K., Fundamentals of Digital Image Processing, Information and Systems Sciences Series, pp. 49–75, Prentice–Hall, Englewood Cliffs, NJ, 1989.

[1] JAHNE B. Digital Image Processing, Concepts , Algorithms and Scientific Applications, Springer Verlag Berlin Heideberg, pp. 482 – 487, 1997.

[2] NAJMAN L. AND M. SCHMITT, Geodesic saliency of watershed contours and hierarchical segmentation, IEEE Trans. Pattern. Anal. Mach. Intell., 18(12), pp. 1163–1173, 1996.

[3] PATRICK DE SMET, RUI LUI´S V. P. M. PIRES, DANNY DE VLEESCHAUWER, IGNACE BRUYLAND Activity driven nonlinear diffusion for color image watershed segmentation, Journal of Electronic Imaging 8(3), July, pp. 270– 278, 1999.

[4] PERONA P., MALIK M., Scale-space and edge detection using anisotropic diffusion, IEEE Trans Pattern. Anal. Mach. Intell. 12(7), pp. 629–639, 1990.

[5] VINCENT L. AND P.SOILLE. Watershed in digital spaces: an efficient algorithm based on immersion simulations. IEEE Trans. on PAMI, 13(6), pp. 583–598, 1991.

[6] WARDROP PJ, SIM S, MCLAREN K. Contact endoscopy of the larynx: a quantitative study. J Laryngol Otol., Jun, 114(6), pp. 437-440, 2000.

[7] WEICKERT J. A review of nonlinear diffusion filtering. In: ScaleSpace, pp. 3–28, 1997.